RSC Advances

TITLE PAGE

Dendrimer Conjugates for Light-activated Delivery of Antisense Oligonucleotides

Ahu Yuan[a,b], Yiqiao Hu[b], and Xin Ming[a,]*

[a] Division of Molecular Pharmaceutics, UNC Eshelman School of Pharmacy, University of North Carolina, Chapel Hill, NC 27599, USA

[b] State Key Laboratory of Pharmaceutical Biotechnology, Nanjing University, Nanjing 210093, China

*Corresponding author: Dr. Xin Ming, E-mail: xming@email.unc.edu, Phone number: 1-919-966-4343, Fax number: 1-919-843-3017.

Abstract:

Therapeutic oligonucleotides, such as splice switching ONs (SSOs), provide opportunity for treating serious, life-threatening diseases. However, the development of ONs as therapeutic agents has progressed slowly, because difficult cytosolic delivery of SSOs into cytosol and nucleus remains a major barrier. Photochemical internalization (PCI), a promising strategy for endosomal escape, was introduced to disrupt the endosomal membrane using light and photosensitizer. Here we constructed Poly(amido amine) (PAMAM) dendrimer conjugates to simultaneously deliver SSOs and photosensitizers into endo/lysosomal compartments. After photo-irradiation, considerable ONs were observed to diffuse to cytosol and accumulate in nucleus. Furthermore, the PCI mediated cytosolic delivery of SSOs effectively enhanced their nuclear splice switching activity.

Key words:

Splice switching oligonucleotides; dendrimers; photosensitizer; photochemical internalization; cytosolic delivery

Abbreviations:

Ce6, Chlorin E6; eGFP, enhanced green fluorescence protein; PAMAM, Poly(amido amine); PCI, photochemical internalization; PMO, phosphorodiamidate morpholino oligomer; SSO, splice switching oligonucleotide.
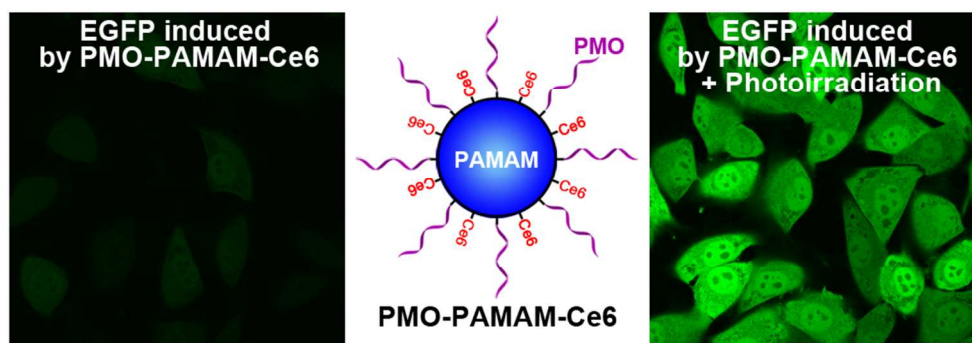
Introduction

There are great interests in the therapeutic oligonucleotides (ONs), such as siRNA and antisense oligonucleotides (ASOs), in treating various diseases.[1-3] Splice switching oligonucleotide (SSO), a type of therapeutic ON, can hybridize to targeted nuclear pre-mRNA and block access of other splicing factors to modulate alternative splicing and subsequent gene expression. SSOs have been tested for treating Duchenne muscular dystrophy in clinical trials and treating cancers in preclinical studies.[4, 5] For instance, a SSO can redirect Bcl-x splicing from anti-apoptotic Bcl-x$_L$ to pro-apoptotic Bcl-x$_S$ and subsequently induce apoptosis of tumor cells.[6, 7] Despite the great potential as novel therapeutic agents, the development of SSOs as therapeutic agents has progressed slowly.[8, 9] A major impediment has been the difficult delivery of these large, hydrophilic and often charged macromolecules from endosomal compartments into cytosol or nucleus of cells.[10] One promising strategy to overcome this intracellular barrier is photochemical internalization (PCI) that disrupts the endosomal membrane using light and photosensitizer (PS).[11-13] Nobuhiro Nishiyama and coworkers suggested that the subcellular localization of PSs might be the key to achieve cytosolic delivery with low non-specific photo-toxicity using PCI approach.[12] When the PSs distributed in photodamage-sensitive organelles such as cytoplasmic membrane and mitochondria, they produced severe photo-toxicity and diminished PCI-mediated cytosolic delivery of therapeutic ONs.[14, 15]

In this study, we aimed to link both ONs and PSs in poly(amido amine) (PAMAM) dendrimer, and thereafter cellular delivery of the dendritic conjugates allows spatiotemporal distribution of the two modalities within endo/lysosomal compartments for superior delivery of ONs. We chose phosphorodiamidate morpholino oligomer (PMO), a third generation of ON, to construct the dendritic conjugates as PMO is a non-charged ON[16, 17] and can decrease the cytotoxicity of the highly positively charged dendrimers. We utilized a reductively responsive disulfide bond to link PMO to PAMAM. Then Ce6 was activated and conjugated to the residual amino on the surface of PAMAM (Fig. 1). Cellular delivery of the dendritic conjugates leads to co-localization of the PMO and Ce6 in the endo/lysosomal compartments. Further light irradiation causes great functional delivery of the PMO.
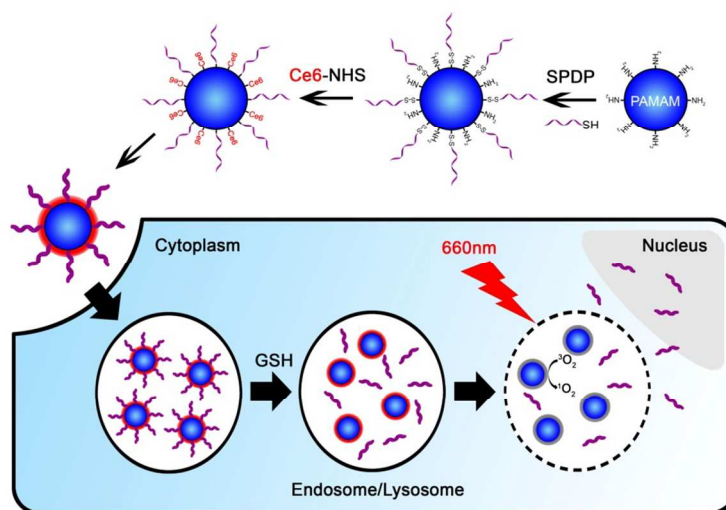
Fig. 1 Preparation of PMO-PAMAM-Ce6 conjugates and schematic illustration showing the process of light-activated endosomal escape of the PMO.

Materials and Methods

Preparation of PMO-PAMAM-Ce6 conjugates

The PMO SSO (5'-GTTATTCTTTAGAATGGTGC-3') was synthesized by Gene Tools, LLC (Philomath, OR, USA). PMO was functionalized with a disulfide amide for sulfhydryl linkage at the 3′ position (PMO-S-S-R). The amino groups of the PAMAM (generation 5.0, Dendritech, Inc.) were reacted with the bifunctional crosslinker *N*-succinimidyl 3-(2-pyridyldithio) propionate (SPDP, Thermo Fisher Scientific) at a 1:25 molar ratio of PAMAM to linker in PBS (1 mM EDTA, pH 7.5) for 1 h at room temperature. The thiol group of PMO was freshly generated by incubating PMO-S-S-R with 10 mM DTT for 1 h at room temperature, and any residual DTT was removed by gel filtration (Sephadex G-25, GE Healthcare). PAMAM-SPDP was then reacted with the thiol group of PMO at the molar ratio of 1:25 in PBS (1 mM EDTA, pH 7.0) overnight, and the product was purified by gel filtration (Sephadex G-100) to obtain PMO-PAMAM.

Ce6 (MedKoo Biosciences Inc.) was dissolved in DMSO, followed by the addition of 10 molar equivalents of EDC and Sulfo-NHS (Thermo Fisher Scientific). After overnight incubation, activated Ce6 (Ce6-NHS) was added to PMO-PAMAM with a 15:1 molar ratio and incubated for 12 hrs in dark at room temperature. After that, the product was purified by gel filtration (Sephadex LH-20, GE Healthcare) to remove unconjugated Ce6, and the mobile phase was mixture of methanol and distilled water (v/v=1:3). Then the solvent was removed under vacuum, the PMO-PAMAM-Ce6 were

redistributed in PBS. The concentration of PMO and Ce6 of PMO-PAMAM-Ce6 conjugates were detected by the 260nm and 403nm absorbance, respectively.

In order to prepare labelled conjugates that were used in flow cytometry and imaging experiments, a PMO that is functionalized with a primary amine at the 5′ position and a disulfide amide for sulfhydryl linkage at the 3′ position was synthesized by Gene Tools, LLC. The PMO was labelled with Alexa Fluor® 488 NHS Ester (Life Technologies) and was referred as PMO_{488}. Then PMO_{488} was used to prepare fluorescent conjugates termed as PMO_{488}-PMO-Ce6.

Physical Characterization of PMO-PAMAM-Ce6 conjugates

The size and zeta potential of PMO-PAMAM-Ce6 was evaluated using a Zetasizer Nano (Malvern Instruments). To test the release profile, PMO-PAMAM-Ce6 conjugates were incubated with PBS containing 10mM glutathione (GSH) at 37°C for 4 h, and PBS was used as a control. After incubation, two samples were eluted by Sephadex G-100 with 0.5ml sample per tube. The PMO concentration in each fraction was detected by Nanodrop 1000 (Thermo Scientific, Wilmington, DE) at 260nm absorbance.

Cellular uptake

A375 cells were cultured in DMEM medium (Life Technologies) containing 10% fetal bovine serum (Sigma). After attachment, the cells were incubated with PMO_{488}-PAMAM-Ce6 (400nM of Ce6) for 12 hrs. Equivalent free PMO_{488} and Ce6 were incubated with cells as well. After that, the cellular uptake was measured by flow cytometry using a LSR II cell analyzer (Becton-Dickenson, CA), with QD655 channel for Ce6 and FITC channel for PMO_{488}.

Subcellular distribution

Intracellular distribution of PMO_{488}-PAMAM-Ce6 in A375 cells was observed using OLYMPUS FV1200 confocal microscope. Fifty thousand cells were seeded on glass coated dishes (MatTek, MA) and incubated for attachment. Subsequently, PMO_{488}-PAMAM-Ce6 (400nM of Ce6) was added into the cells for 12-h incubation. After that, cells were observed by confocal microscopy, with QD655 channel for Ce6 and Alexa 488 channel for PMO_{488}. In addition, intracellular distribution of PMO_{488}-PAMAM and free Ce6 (5µM) was detected by confocal as well. Lysotracker Red was used to detect the subcellular distribution of PMO_{488}-PAMAM-Ce6 in A375 cells. Cells were treated with PMO_{488}-PAMAM-Ce6 (400nM of Ce6) for 12 hrs, followed by incubation with 100nM Lysotracker Red for 1 h prior to confocal imaging. Alexa 488 channel was used for detection of PMO_{488}, and Alexa 594 channel was used for Lysotracker Red.

Light activated endosomal release

Confocal imaging was performed to detect the PCI mediated endosomal release of PMO_{488}-PAMAM-Ce6 upon photo-irradiation. A375 cells were seeded on glass coated dishes and incubated for attachment. PMO_{488}-PAMAM-Ce6 (50nM of Ce6) was added and incubated for 12 hrs. After that, cells were washed twice with fresh media and photo-irradiated for 20min. After incubation with another 12 hrs, the cells were imaged by confocal microscopy, and the images were collected with a 60× oil immersion lens.

PCI induced eGFP expression

A375/eGFP654 cells were seeded on 48-well plates at the density of 30,000 cells per well. After one day, cells were treated by free PMO (125nM) and PMO-PAMAM-Ce6 (50nM of Ce6 and 125nM of PMO). After 12-h treatment, cells were washed twice with fresh media. After that, cells treated by PMO-PAMAM-Ce6 were photo-irradiated by a 660nm laser for 20min. After a day, cells were trypsinized and their eGFP expression was detected by flow cytometry. Cells treated by PBS were set as negative control and cells treated by Lipofectamine 2000 (L2K) complexes of negatively charged phosphorothioate ONs (the same concentration and sequence) were set as positive control. The cell viability of A375/eGFP654 cells after the same treatments was examined using Alamar Blue assay (Life Technologies). eGFP expression in A375/eGFP654 cells was also observed by confocal imaging using OLYMPUS FV1200.

Data analysis

Data are expressed as mean ± SD from three measurements unless otherwise noted. Statistical significance was evaluated using *t*-test for two-sample comparison or ANOVA followed by Dunnet's test for multiple comparisons. The data were analyzed with GraphPad Prism 5 (GraphPad Software, Inc., La Jolla, CA).

Results

Preparation and characterization of PMO-PAMAM-Ce6 conjugates

PAMAM was modified with SPDP and then reacted with the thiol group at the 3' end of PMO. The obtained products were purified with Sephadex G-100 column to remove unreacted PMO. NHS activated Ce6 was conjugated to PMO-PAMAM to obtain PMO-PAMAM-Ce6, and the conjugates were further purified with Sephadex LH-20 (Fig.S1). The molar ratio of PMO to Ce6 on PMO-PAMAM-Ce6 conjugates was demonstrated as 2.5:1, according to the absorbance in 260nm and 403nm, respectively (Fig.S1).

The diameter of PMO-PAMAM-Ce6 conjugates is 21.1nm (Fig.S2), measured by dynamic light scattering (DLS). The zeta potential of PMO-PAMAM-Ce6 conjugates is +2.2mV (Fig.S3). The significant decrease of zeta potential from about +17mV of PAMAM to +2.2mV of PMO-PAMAM-Ce6 are primarily due to the amine blocking and the modification of PMO and Ce6 molecules.

Next we tested whether intracellular sulfhydryl can release the PMOs from the PMO-PAMAM-Ce6 conjugates using PBS containing 10mM GSH (Fig. 2). In gel filtration (Sephadex G-100 column) of the GSH treated sample, 85.9% of PMOs were eluted slower (between 16 to 30 fractions) and were separated from the conjugates content (between 4 to 11 fractions), indicating that the majority of PMOs could be cleaved from the conjugates in the cellular reducing environment.
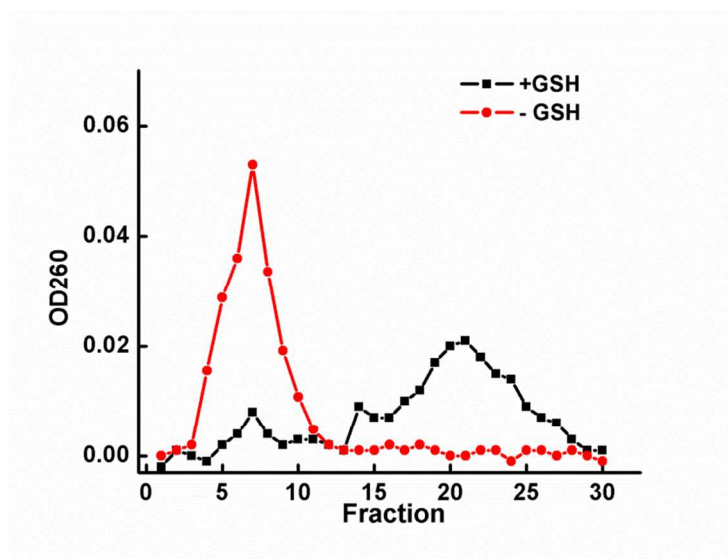

Fig. 2 PMOs release profile from PMO-PAMAM-Ce6 by 10mM Glutathione.

Cellular uptake

To compare the cellular uptake of PMO-PAMAM-Ce6 conjugates to free PMOs and Ce6, we labelled fluorescent Alexa-488 to PMO, and then successively conjugated PMO_{488} and Ce6 to PAMAM. Cellular uptake was evaluated by incubating cells with PMO_{488}, free Ce6 and PMO_{488}-PAMAM-Ce6, followed by flow cytometry (Ex 488nm, Em 525/20nm for PMO_{488}; Ex 405nm, Em 655/20 for Ce6). As shown in Fig. 3, Free PMO_{488} did not enter into the cells significantly, but the dendritic conjugates showed substantial cellular uptake (Fig. 3A). Similarly, the Ce6 fluorescence from PMO_{488}-PAMAM-Ce6 was also significantly higher than that of free Ce6 group (Fig. 3B). These results indicated that the conjugation of PMO and Ce6 to PAMAM together facilitated their internalization, which might be contributed to effective intracellular internalization of PAMAM dendrimers.[18, 19]
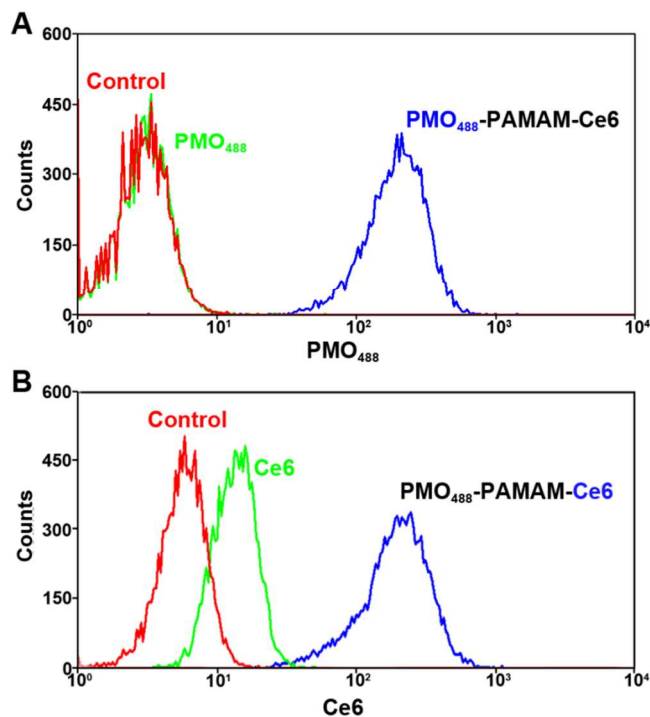
Fig. 3 Comparison of cellular uptake of PMO-PAMAM-Ce6 to free PMO and Ce6 in A375 cells. Alexa Fluor® 488 was labelled to PMO to form PMO_{488}-PAMAM-Ce6. (A) Cellular uptake of PMOs in FITC channel. Red: Control, Green: Free PMO_{488} and Blue: PMO_{488}-PAMAM-Ce6. (B) Cellular uptake of Ce6 in QD655 channel. Red: Control, Green: Free Ce6 and Blue: PMO_{488}-PAMAM-Ce6.
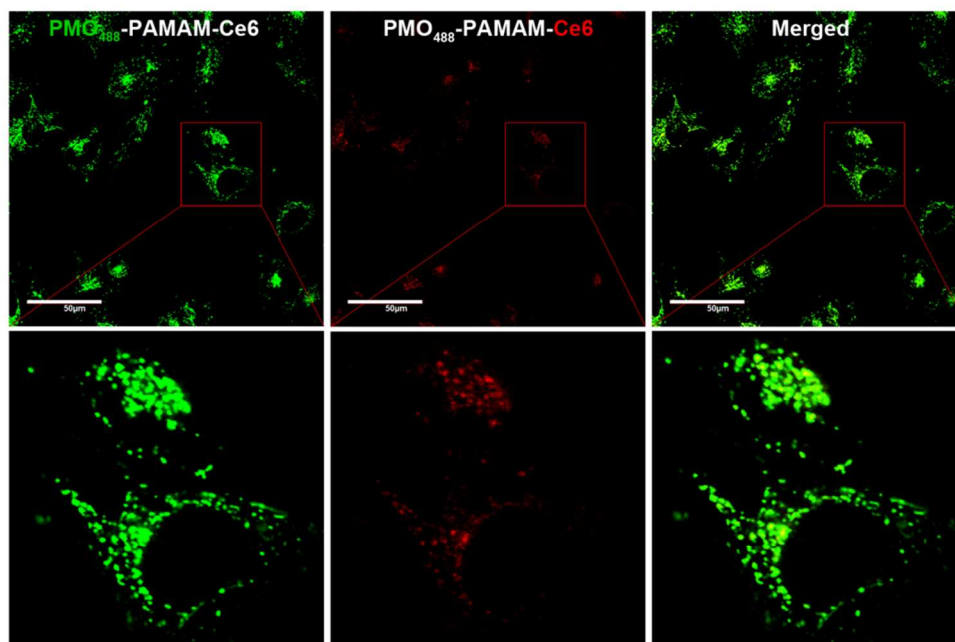

Fig. 4 Colocalization of PMO_{488} and Ce6 in A375 cells. Cells were incubated with PMO_{488}-PAMAM-

Ce6 for 12 hours. Scale bars, 50μm.

Intracellular distribution of PMO-PAMAM-Ce6 conjugates

Following cellular internalization, the spatial distribution of PMO$_{488}$ and Ce6 after 12-h incubation with PMO$_{488}$-PAMAM-Ce6 conjugates was observed using confocal imaging. The images demonstrated that red punctate fluorescence of Ce6 completely colocalized with green fluorescence of PMO$_{488}$ in the cytoplasm (Fig. 4). However, in the cells treated with PMO$_{488}$-PAMAM and free Ce6, diffused red Ce6 fluorescence merely exhibited partial colocalization with green PMO$_{488}$ (Fig.S4). We quantified the colocalization between PMO$_{488}$ and Ce6 using Pearson's correlation coefficient (PCC). In the PMO$_{488}$-PAMAM-Ce6 conjugates group, the PCC value was 0.76, which was significantly higher than that in PMO-PAMAM with free Ce6 group (PCC=0.283, $p<0.001$, Fig.S5). These results confirmed their spatiotemporal co-localization of the two modalities. The complete colocalization between ONs and PSs provided the possibility for superior cytosolic delivery of ONs as well as reduced photo-toxicity. In addition, intracellular localization of the fluorescent conjugates was also detected with Lysotracker. Green fluorescent punctuates of conjugates were largely colocalized with Lysotracker Red, indicating that PMO$_{488}$-PAMAM-Ce6 located in the acidic vesicular organelles, including late endosomes and lysosomes (Fig.S6).
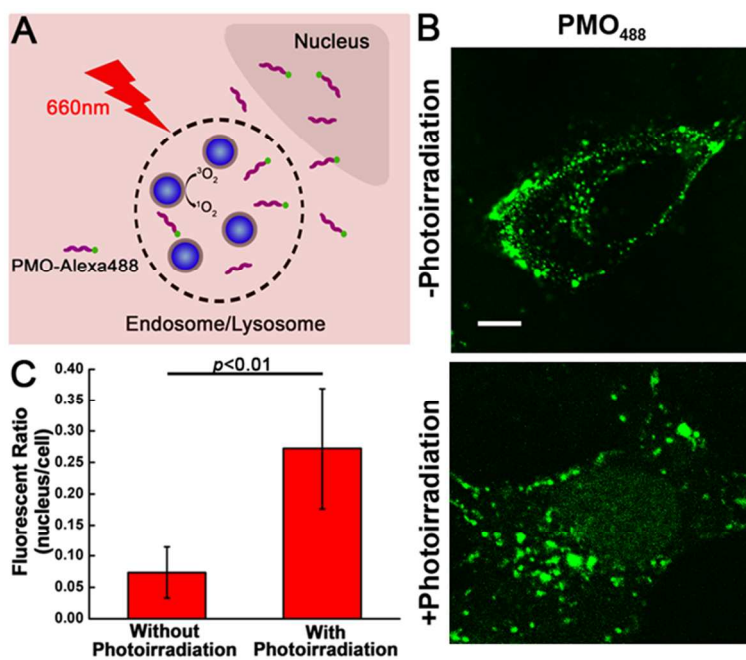

Fig. 5 (A) Schematic diagram of PCI mediated of cytosolic delivery of fluorescent PMOs. (B) Re-distribution of released PMO$_{488}$ from PMO$_{488}$-PAMAM-Ce6 without (upper) or with (below) photo-

irradiation in A375 cells. Scale bars, 5µm. (C) Quantification of the percentage of nuclear fluorescent signal to whole cells. The percentage was shown as mean and standard deviation obtained from 10 cells.

Next, we examined the light-activated delivery of ONs to nucleus, where PMO interacts with its target pre-mRNA (Fig. 5A). Without photo-irradiation, fluorescent PMO was confined to endo/lysosomal compartments without obvious fluorescent signal in cytosol and nucleus. However, in the cells treated with PMO_{488}-PMO-Ce6 and followed by photo-irradiation, diffused green fluorescence was observed in the cytosol and nucleus region (Fig. 5B). The percentage of nuclear fluorescent signal to the whole cells significantly increased from 6.7% to 27% when cells were photo-irradiated (Fig. 5C).
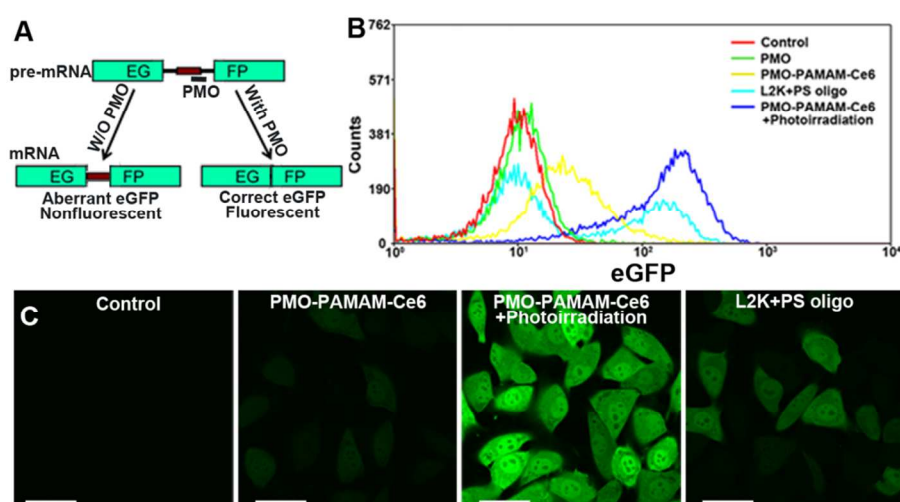

Fig. 6 Induction of eGFP by PMO-PAMAM-Ce6 with or without photo-irradiation. (A) The eGFP cDNA (green) is interrupted by an aberrantly spliced intron in which a portion (red) is spliced into the mRNA, producing aberrant eGFP (nonfluorescent). Blocking the aberrant splice site within the intron with a PMO prevents aberrant splicing and restores the reading frame of the eGFP to produce wild-type eGFP (fluorescent).[20-22] (B) Flow cytometry of eGFP expression in A375/eGFP654 cells treated with free PMO, PMO-PAMAM-Ce6 with or without photo-irradiation. PBS treatment was set as a negative control and L2K/ PS ON complexes treatment was set as positive control. (C) Confocal images of A375/eGFP654 cells treated by PMO-PAMAM-Ce6 with or without photo-irradiation and L2K/ PS ON complexes. Bar=50µm.

PCI mediated eGFP induction

Finally, functional delivery by PMO-PAMAM-Ce6 followed by photo-irradiation was examined by flow cytometry and confocal imaging (Fig. 6). A375 cells were stably transfected with eGFP

expression cassettes containing a mutated intron and were referred as A375/eGFP654 cells. A model SSO targets an intronic splice site and causes splicing out of the intron and expression of wild-type eGFP protein (Fig. 6A).[20-22] eGFP induction of A375/eGFP654 cells without any treatment was set as control. A375/eGFP654 cells treated by free PMO (125nM) did not induce eGFP expression as the fluorescent peak coincides with the negative control. Compared with the negative control, the mean eGFP fluorescence of cells treated by PMO-PAMAM-Ce6 (PMO 125nM; Ce6 50nM) with or without photo-irradiation increased by 18.9- and 2.8- fold, respectively. PMO-PAMAM-Ce6 significantly increased functional delivery of the SSO in a light-activated manner (Fig. 6B). In addition, the cells treated with Lipofectamine 2000(L2K) complexes of PS ON (125nM) exhibited 5.9-fold eGFP induction, which was significantly lower than that of the PMO-PAMAM-Ce6 with photo-irradiation group (Fig.S7). Meanwhile, nearly 92% of cells treated by PMO-PAMAM-Ce6 with photo-irradiation were induced to express eGFP, in comparison with 39.2% in cells treated with L2K/PS ONs (Fig.S8). Moreover, these flow data was confirmed by the confocal images (Fig. 6C). In control group, no obvious green fluorescence could be observed. Cells treated by PMO-PAMAM-Ce6 exhibited dim green fluorescence. However, strong green fluorescence was observed in almost all the cells in the PMO-PAMAM-Ce6 plus photo-irradiation group. These results strongly suggested that dendritic conjugates can produce effective delivery of ONs after photo-irradiation.

Discussion

PMO is a type of third generation ONs and has exhibited excellent chemical stability and resistance to nucleases and proteases in vitro and in vivo.[23] PMO has been tested as a therapeutic agent in both animal models and human clinical trials.[24, 25] However, in these applications, high dose of PMOs is needed to achieve these positive therapeutic outcomes. Poor cellular uptake [8] and insufficient endosomal escape [13] are two main causes for this clinical predicament. PMOs must be delivered to the cytosol of target cells to produce pharmacological actions. Once in the cytosol, PMOs can freely diffuse between the cytosol and nucleus. To facilitate the internalization, we conjugate multiple PMOs onto the positive charged PAMAM dendrimers. For effective endosomal release of PMOs, we introduce PS Ce6 to PMO-PAMAM conjugates to obtain PMO-PAMAM-Ce6 for photochemical internalization (PCI). There are some advantages for the simultaneous conjugation of PMOs and Ce6: (1) facilitating the internalization of these two modalities into cells; (2) guaranteeing their spatiotemporally colocalization in endo/lysosomal compartments; (3) avoiding the distribution of PSs in photo-damage sensitive

organelles, including cytoplasmic membrane and mitochondria. These features have led to the effective light-activated cytosolic delivery of ONs as well as reduced phototoxicity.

We selected PAMAM dendrimers for co-delivery of PMOs and Ce6 because of three advantages of PAMAM dendrimers over linear polymers such as polyethylenimine. Firstly, PAMAM dendrimers have more surface amine groups than linear PEI polymers for linking ONs and PSs. Secondly, PAMAM dendrimers are monodisperse macromolecules, unlike linear polymers. Thus, we can obtain homogenous conjugates by using dendrimers. Third, linear chains exist as flexible coils in solution; while dendrimers form a tightly packed ball. The globular architecture of the dendrimers makes their end groups more accessible for conjugation of cargo molecules.

The cytotoxicity of the photo-irradiation could be observed during the process of PCI. In the absence of photo-irradiation, PMO-PAMAM-Ce6 did not show obvious dark cytotoxicity. While upon photo-irradiation, the efficient PCI mediated cytosolic delivery was accompanied with approximately 20% decrease in the cell viability (Fig.S9). Compared with Lipofectamine 2000 (L2K), PMO-PAMAM-Ce6 conjugates plus photo-irradiation caused similar cytotoxicity, but significant higher induced eGFP expression (Fig.S7 and S9). During the PCI, endo/lysosomal membranes are destructed by ROS to release ONs. Meanwhile, leakage of some cytotoxic lysosomal proteases into cytosol is inevitable.[26]

In summary, we constructed dendritic conjugates to simultaneously deliver ONs and PSs into endo/lysosomal compartments. Upon light activation, PMOs are delivered to the nucleus and then bind to the target pre-mRNA. Furthermore, light-activated delivery using our dendritic conjugates has achieved functional delivery of ONs that is superior to the gold standard Lipofectamine transfection. To our best knowledge, this has been the first study of using dendrimers to prepare ON conjugates for light-activated delivery of ONs, and this study may thus provide a novel approach for functional delivery of therapeutic ONs including siRNAs, antisense ONs, SSOs, and antagomirs to microRNAs and long non-coding RNAs.

RSC Advances Accepted Manuscript

Reference:

1. J. E. Dahlman, C. Barnes, O. F. Khan, A. Thiriot, S. Jhunjunwala, T. E. Shaw, Y. Xing, H. B. Sager, G. Sahay, L. Speciner, A. Bader, R. L. Bogorad, H. Yin, T. Racie, Y. Dong, S. Jiang, D. Seedorf, A. Dave, K. Singh Sandhu, M. J. Webber, T. Novobrantseva, V. M. Ruda, A. K. Lytton-Jean, C. G. Levins, B. Kalish, D. K. Mudge, M. Perez, L. Abezgauz, P. Dutta, L. Smith, K. Charisse, M. W. Kieran, K. Fitzgerald, M. Nahrendorf, D. Danino, R. M. Tuder, U. H. von Andrian, A. Akinc, D. Panigrahy, A. Schroeder, V. Koteliansky, R. Langer and D. G. Anderson, *Nature nanotechnology*, 2014, **9**, 648-655.

2. K. Y. Choi, O. F. Silvestre, X. Huang, N. Hida, G. Liu, D. N. Ho, S. Lee, S. W. Lee, J. I. Hong and X. Chen, *Nature protocols*, 2014, **9**, 1900-1915.

3. K. A. Whitehead, J. R. Dorkin, A. J. Vegas, P. H. Chang, O. Veiseh, J. Matthews, O. S. Fenton, Y. Zhang, K. T. Olejnik, V. Yesilyurt, D. Chen, S. Barros, B. Klebanov, T. Novobrantseva, R. Langer and D. G. Anderson, *Nat Commun*, 2014, **5**, 4277.

4. P. Disterer, A. Kryczka, Y. Liu, Y. E. Badi, J. J. Wong, J. S. Owen and B. Khoo, *Human gene therapy*, 2014, **25**, 587-598.

5. J. Bauman, N. Jearawiriyapaisarn and R. Kole, *Oligonucleotides*, 2009, **19**, 1-13.

6. J. A. Bauman, S. D. Li, A. Yang, L. Huang and R. Kole, *Nucleic acids research*, 2010, **38**, 8348-8356.

7. J. Roberts, E. Palma, P. Sazani, H. Orum, M. Cho and R. Kole, *Molecular therapy : the journal of the American Society of Gene Therapy*, 2006, **14**, 471-475.

8. X. Ming, K. Carver and L. Wu, *Biomaterials*, 2013, **34**, 7939-7949.

9. P. Grabowski, *Nat Biotechnol*, 2002, **20**, 346-347.

10. J. Winkler, *Therapeutic delivery*, 2013, **4**, 791-809.

11. G. Pasparakis, T. Manouras, M. Vamvakaki and P. Argitis, *Nat Commun*, 2014, **5**, 3623.

12. N. Nishiyama, A. Iriyama, W. D. Jang, K. Miyata, K. Itaka, Y. Inoue, H. Takahashi, Y. Yanagi, Y. Tamaki, H. Koyama and K. Kataoka, *Nature materials*, 2005, **4**, 934-941.

13. T. Nomoto, S. Fukushima, M. Kumagai, K. Machitani, Arnida, Y. Matsumoto, M. Oba, K. Miyata, K. Osada, N. Nishiyama and K. Kataoka, *Nat Commun*, 2014, **5**, 3545.

14. M. Mitsunaga, M. Ogawa, N. Kosaka, L. T. Rosenblum, P. L. Choyke and H. Kobayashi, *Nature medicine*, 2011, **17**, 1685-1691.

15. S. Marrache, S. Tundup, D. A. Harn and S. Dhar, *Acs Nano*, 2013, **7**, 7392-7402.

16. R. G. Panchal, B. L. Geller, B. Mellbye, D. Lane, P. L. Iversen and S. Bavari, *Nucleic acid therapeutics*, 2012, **22**, 316-322.

17. F. Muntoni and M. J. Wood, *Nature reviews. Drug discovery*, 2011, **10**, 621-637.

18. S. Parimi, T. J. Barnes, D. F. Callen and C. A. Prestidge, *Biomacromolecules*, 2010, **11**, 382-389.

19. M. Akin, R. Bongartz, J. G. Walter, D. O. Demirkol, F. Stahl, S. Timur and T. Scheper, *J Mater Chem*, 2012, **22**, 11529-11536.

20. M. R. Alam, X. Ming, V. Dixit, M. Fisher, X. Chen and R. L. Juliano, *Oligonucleotides*, 2010, **20**, 103-109.

21. M. R. Alam, V. Dixit, H. Kang, Z. B. Li, X. Chen, J. Trejo, M. Fisher and R. L. Juliano, *Nucleic acids research*, 2008, **36**, 2764-2776.

22. X. Ming, K. Carver, M. Fisher, R. Noel, J. C. Cintrat, D. Gillet, J. Barbier, C. Cao, J. Bauman and R. L. Juliano, *Nucleic acids research*, 2013, **41**, 3673-3687.

23. J. H. Chan, S. Lim and W. S. Wong, *Clinical and experimental pharmacology & physiology*, 2006, **33**, 533-540.

24. G. R. Devi, T. M. Beer, C. L. Corless, V. Arora, D. L. Weller and P. L. Iversen, *Clinical cancer research : an official journal of the American Association for Cancer Research*, 2005, **11**, 3930-3938.

25. B. Wu, C. Cloer, P. Lu, S. Milazi, M. Shaban, S. N. Shah, L. Marston-Poe, H. M. Moulton and Q. L. Lu, *Gene therapy*, 2014, **21**, 785-793.

26. N. H. Petersen, O. D. Olsen, L. Groth-Pedersen, A. M. Ellegaard, M. Bilgin, S. Redmer, M. S. Ostenfeld, D. Ulanet, T. H. Dovmark, A. Lonborg, S. D. Vindelov, D. Hanahan, C. Arenz, C. S. Ejsing, T. Kirkegaard, M. Rohde, J. Nylandsted and M. Jaattela, *Cancer cell*, 2013, **24**, 379-393.